57. GABA-mediated IPSPs: Y. Ben-Ari, K. Krnjevic, W. Reinhardt, *Can. J. Physiol. Pharmacol.* **57**, 1462 (1979); R. Wong and D. Watkins, *J. Neurophysiol.* **48**, 938 (1982); M. McCarren and B. Alger, *ibid.* **53**, 557 (1985). Glycine-mediated IPSPs: H. Korn *et al.*, *J. Neurosci.* **4**, 125 (1984).
58. K. Krnjevic, in *Physiology and Pharmacology of Epileptogenic Phenomena*, M. Klee, D. Lux, E. Speckman, Eds. (Raven, New York, 1982), pp. 123–130; D. Barnes and M. Dichter, *Soc. Neurosci. Abstr.* **10**, 419 (1984).
59. M. Frosch, thesis, Harvard University (1987).
60. R. Traynelis and R. Dingledine, *Soc. Neurosci. Abstr.* **12**, 74 (1986).
61. B. Connors and R. Chervin, *ibid.*, p. 350; R. Chervin and B. Connors, *ibid.*, p. 350.
62. M. A. Mirski and J. A. Ferrendelli, *Science* **226**, 72 (1984); *Epilepsia* **25**, 661 (1984); J. Miller and J. Ferrendelli, in *Mechanisms of Epilepsy: The Transition to Seizure*, M. Dichter, Ed. (Plenum, New York, in press).
63. S. Piredda, C. Lim, K. Gale, *Life Sci.* **36**, 1295 (1985).
64. S. Piredda and K. Gale, *Nature (London)* **317**, 623 (1985).
65. M. J. Iadarola and K. Gale, *Mol. Cell. Biochem.* **39**, 305 (1981); *Science* **218**, 1237 (1982); G. Le Gal La Salle, M. Kijima, S. Feldblum, *Neurosci. Lett.* **36**, 69 (1983); J. McNamara, L. Rigsbee, M. Galloway, *Eur. J. Pharmacol.* **86**, 485 (1983); J. McNamara, M. Galloway, L. Rigsbee, C. Shin, *J. Neurosci.* **4**, 2410 (1984).
66. D. Garant and K. Gale, *Brain Res.* **273**, 156 (1983); K. Gale, *Fed. Proc. Fed. Am. Soc. Exp. Biol.* **44**, 2414 (1985).
67. D. Garant and K. Gale, *Soc. Neurosci. Abstr.* **12**, 80 (1986).
68. G. Goddard, *Nature (London)* **214**, 1020 (1967); R. Racine, *Neurosurgery* **3**, 234 (1978); J. McNamara *et al.*, *Crit. Rev. Clin. Neurobiol.* **1**, 341 (1985).
69. G. King *et al.*, *J. Neurophysiol.* **54**, 1295 (1985); W. Wadman *et al.*, *Exp. Brain Res.* **57**, 404 (1985); D. McIntyre and R. Wong, *Exp. Neurol.* **88**, 529 (1985); *J. Neurophysiol.* **55**, 1295 (1986); S. Piredda *et al.*, *Exp. Neurol.* **90**, 659 (1986); J. McNamara, D. Bonhaus, C. Shin, in *Mechanisms of Epilepsy: The Transition to Seizure*, M. Dichter, Ed. (Plenum, New York, in press).
70. J. Engel and C. Wilson, in *Neurotransmitters, Seizures, and Epilepsy III*, P. L. Morselli, G. Nistico, K. G. Lloyd, R. G. Fariello, J. Engel, Jr., Eds. (Raven, New York, 1986), pp. 1–13.
71. B. E. Alger and R. A Nicoll, *Science* **210**, 1122 (1980).
72. P. A. Schwartzkroin and C. E. Stafstrom, *ibid.*, p. 1125.
73. J. Hablitz, *Neurosci. Lett.* **22**, 159 (1981).

Research Articles

Laser-Stimulated Luminescence Used to Measure X-ray Diffraction of a Contracting Striated Muscle

YOSHIYUKI AMEMIYA, KATSUZO WAKABAYASHI, HIDEHIRO TANAKA, YUTAKA UENO, JUNJI MIYAHARA

An integrating x-ray area detector that operates on the basis of laser-stimulated luminescence was used in a diffraction study of muscle contraction. The area detector has a dynamic range of 1 to 10^5, a sensitivity about 60 times greater with approximately 1/300 as much fog background as x-ray film. It is erasable and reusable but, like film, can integrate at a practically unlimited counting rate. The high sensitivity and wide dynamic range of the detector resulted in a sufficient reduction in the exposure time to make possible the recording of a clear x-ray diffraction pattern, with up to 2.0-nanometer axial spacing, from a contracting frog skeletal muscle in as little as 10 seconds with synchrotron radiation. During the isometric contraction of the muscle, most of the actin diffraction lines increased in intensity without noticeable changes in their peak positions. Changes also occurred in diffraction intensities from the myosin heads. The results indicate that during contraction the structure of the actin filaments differs from that in the rigor state, suggesting a possible structural change in the actin subunits themselves; the myosin heads during contraction retain the axial periodicity of the myosin filament and become aligned in a more perpendicular manner to the actin filaments.

X-RAY DIFFRACTION PATTERNS FROM CONTRACTING MUSCLES have been previously studied with synchrotron radiation in the time-resolved mode with gas-type one-dimensional detectors (*1–6*). These studies have provided information on the molecular changes that occur during force development and sliding movement. The approach complementary to the time-resolved structure analysis has been to study the entire two-dimensional diffraction pattern at high spatial resolution with area detectors. Such experiments had been performed by recording on film the patterns from a long series of contractions (*7–9*). However, the exposure time required for satisfactory patterns was too long, and physiological fatigue in the contracting muscle could not be avoided. X-ray television (*1, 10*) and pulse-type area detectors, such as multiwire proportional chambers (MWPC) (*11, 12*), are now being used for this purpose; thus, the required exposure time has become much shorter. These methods still do not overcome several problems. The dynamic range of x-ray television is insufficient, and the spatial distortion and nonuniformity of response cannot be neglected. The spatial resolution of MWPC is not satisfactory and the counting-rate limitation prohibits an effective use of a high x-ray flux of synchrotron radiation.

A storage phosphor screen, called "an imaging plate," and an imaging system in which it is used were recently developed for diagnostic radiography (*13*). This imaging plate is a new type of integrating area detector that can record the diffraction of synchrotron radiation during muscle contraction. We were able to measure intensity changes of weak reflections that have the periodicity of the actin filament.

New integrating area detector. The detector system comprises (i) a phosphor screen (the imaging plate), (ii) an image reader, (iii) an image processor, and (iv) an image writer (Fig. 1). The imaging plate (IP) is a flexible plastic plate coated with a 0.15-mm-thick layer

Y. Amemiya is at the Photon Factory, National Laboratory for High Energy Physics, Oho-machi, Tsukuba-gun, Ibaraki 305, Japan. K. Wakabayashi and Y. Ueno are at the Department of Biophysical Engineering, Faculty of Engineering Science, Osaka University, Toyonaka, Osaka 560, Japan. H. Tanaka is at the Department of Physiology, School of Medicine, Teikyo University, Itabashi-ku, Tokyo 173, Japan. J. Miyahara is a senior research staff of the Miyanodai Development Center, Fuji Photo Film Company Limited, Kaisei-machi, Ashigarakami-gun, Kanagawa 258, Japan.

of fine phosphor crystals ($BaFBr:Eu^{2+}$) (*14*). When exposed to x-rays, the phosphor stores a fraction of the absorbed x-ray energy in the form of quasistable color centers; when they are later stimulated by visible or infrared light, they emit photostimulated luminescence (PSL) (*14*) with an intensity proportional to the number of absorbed x-ray photons. The x-ray image temporarily stored in the phosphor screen is read by the image reader with a focused helium-neon laser beam to scan the screen surface. The emitted PSL is collected by a photomultiplier tube, and the tube output is logarithmically amplified in order to cover the wide dynamic range of the PSL and is then converted with an analog-to-digital converter into a time series of digital signals (8 bits per pixel). The resulting digital data are manipulated by the image processor. The image writer then converts the digital signals back into analog signals that modulate the intensity of another helium-neon laser beam that scans photographic film to record the x-ray image (Fig. 2). The stored image on the IP can be easily erased by irradiation with visible light; this allows repeated use. The IP used in our work had a square face of dimensions 185 by 185 mm^2. The pixel size was 0.1 by 0.1 mm^2 and the scanning speed of laser beam was 14 μsec per pixel. The spatial resolution was about 150 μm at full width of half maximum (FWHM) in two orthogonal directions (*15, 16*). The measured detector quantum efficiency (DQE) (*17*) of the IP for 8-keV x-rays is more than 70 percent; it is several orders of magnitude greater than conventional high-sensitivity x-ray film at lower exposures (*18*). This is because the absorption efficiency of the phosphor is high (~100 percent for 8-keV x-rays) and the background level (~3 photons per pixel) is much lower (~1000 photons per pixel for x-ray film) due to the lack of intrinsic chemical fogs (*15, 18*). The nonuniformity of response is less than 1.6 percent over the area of the plate. The IP has a dynamic range of five orders of magnitude, which is much greater than that of x-ray film (~2.5 orders of magnitude) and x-ray vidicons (approximately three orders of magnitude). The sensitivity of the IP is linear over 3.5 orders of magnitude in the dynamic range. Such a high sensitivity and a wide dynamic range of the IP make it possible to record the entire diffraction pattern from a muscle on a single IP in a short time.

X-ray diffraction from a contracting muscle. We used this system for studying diffraction patterns from a contracting skeletal muscle with synchrotron radiation from a storage ring (Fig. 1). The sartorius muscle of a bullfrog (~6 mm wide and ~1 mm thick) was mounted in a double-focusing x-ray camera (*19, 20*). The incident flux of x-rays (wavelength, $\lambda = 0.155$ nm) on the specimen was approximately 8×10^{10} photons per second when the storage ring was operated at 2.5 GeV with a beam current of 145 mA. The recording exposure time ranged from 5 seconds for strong actin layer lines to 10 seconds for much weaker high-angle actin layer lines of up to ~2.7-nm spacing. This is a great improvement over the 5 to 10 minutes required for recording a visually similar pattern on x-ray film under the same conditions. The muscle was isometrically tetanized at a sarcomere length of about 2.4 μm (nearly the full overlap length of the thin and thick filaments) for 1.3 seconds; this was repeated ten times every 15 seconds. The diffraction pattern (Fig. 2B) was repeatedly recorded ten times with a 1.0-second exposure time during steady tension. Thus, the total exposure time was 10 seconds. The pattern during a resting period (Fig. 2A) was recorded for the same muscle before contraction in the same exposure time. There appeared strong 5.9- and 5.1-nm actin layer lines; except for these two reflections, the actin layer lines are extremely weak. The strong layer-line series with a repeat of 42.9 nm (which appeared like breastbones in the region inside the 5.9-nm actin layer line) are due to the regular helical arrangement of the myosin heads around the thick filament backbone. In contrast, the myosin off-meridional layer lines disappeared and the actin layer lines were distinctly observed (Fig. 2B).

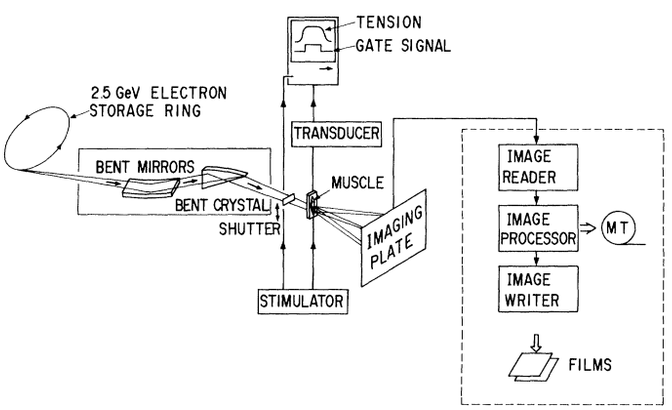

Fig. 1. Experimental configuration for recording two-dimensional x-ray diffraction patterns from contracting muscles with a scanning laser-stimulated photoluminescence system (SLSL system) and synchrotron radiation. Synchrotron x-ray radiation from the 2.5-GeV electron storage ring of the Photon Factory was vertically focused by seven 20-cm-long mirrors (fused silica) and horizontally by a bent crystal monochromator [germanium (111), asymmetry cut-angle = 8°] (*19*). X-ray wavelength was 0.155 nm. The SLSL system (*13*) consists of an imaging plate, an image reader, an image processor, and an image writer. Muscle tension was produced by electrical stimulation and gate signals for an x-ray beam shutter were monitored and recorded with a storage oscilloscope (Tektronix, model 5110).

Changes of actin layer lines during contraction. Figure 2B shows several layer lines which range from the first layer line at ~41-nm spacing to the first meridional layer line at ~2.7-nm spacing. To show the intensity change of the actin layer lines during contraction, we subtracted the digital data of the resting pattern from that of the contracting pattern (Fig. 3). As can be seen in Fig. 3, the diffraction intensities of most of the actin layer lines (now indexed by reciprocal spacings) increased. For instance, the intensity of the 2.7-nm meridional reflection that corresponds to the axial repeat of actin monomers in F-actin increased by about 15 percent. The prominent 5.1- and 5.9-nm reflections increased in the integrated intensity by ~100 percent and 20 to 50 percent, respectively (Fig. 4). These reflections correspond to the pitches of the two helices of the actin monomers in the filament. These changes agreed with previous reports (*3, 5, 6*). There were other layer-line reflections in several places on the row lines located between 0.15 nm^{-1} and 0.3 nm^{-1} from the meridian (Fig. 3). The largest intensification of these reflections was observed on the layer line at an axial spacing of ~1/19 nm^{-1}, corresponding to the second actin layer line. The resting intensity of this reflection was too weak to measure. Its integrated intensity during contraction was about 40 percent of that of the 5.9-nm reflection.

The strong appearance of this reflection has been attributed to a structural change of the tropomyosin in the thin filament on activation (*5, 21, 22*). The first layer line that corresponds to the crossover repeat of the double strands of the F-actin helix was weak and difficult to distinguish from the remnant of the first myosin layer line. Thus, the change was not clear in the inner side; however, a slight and distinct intensification was noted in the radial range of 0.2 to 0.3 nm^{-1}. The axial spacing of the first layer line was about 41 nm, not 37 nm as observed in the rigor muscle, when measured at the radial range below 0.13 nm^{-1} (Fig. 3) after the background intensity is subtracted. However, most of the actin layer lines did not appreciably change shapes or peak positions in the radial direction, nor were their axial spacings significantly different from those in the resting state. As an example, a comparison of the intensity contour maps around the 5.9- and 5.1-nm layer lines is shown in Fig. 4 together with the intensity profiles of the 5.9- and

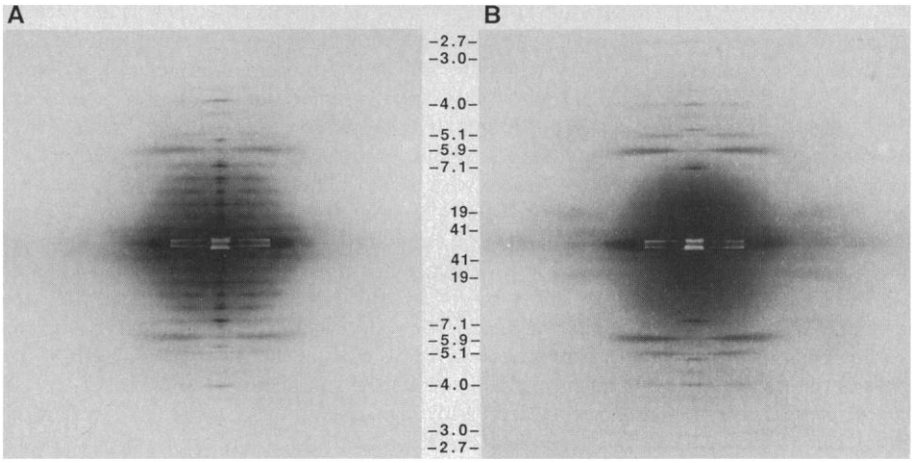

Fig. 2. X-ray diffraction patterns from (**A**) resting state and (**B**) isometrically contracting state of a frog skeletal muscle recorded with imaging plates. Exposure time was 10 seconds; specimen-to-imaging plate distance was 146 cm; fiber axis was along the vertical. Photographs were reduced by a factor of 3. Numbers are axial spacings (in nanometers) of the actin layer lines. The intensity ratio of the (1,1) equatorial reflections in the contracting to resting states was about 2.4. This value indicates that the muscle was fully activated in the contracting pattern (*30*). Actin layer lines in (**B**) tended to become slightly sharper in the axial direction. The first layer line observed at ~41-nm spacing in (**B**) is difficult to distinguish from the first myosin layer-line remnant in (**A**). Three meridional reflections indexed to the first to third orders of a 38.5-nm repeat were present separately from the other actin layer lines, showing a troponin repeat (*21*). The intensity on the equator in the central part was attenuated by approximately a factor of 10 with a copper foil 50 μm thick, 3 mm wide, and 40 mm long glued to a lead beam stop; the signal was not beyond the dynamic range of the imaging plate. The image reader was preset to have full range of digital signals (0 to 255) correspond to 3.6 orders of magnitude of x-ray intensities; thus, the detective quantum efficiency was maximized.

5.1-nm reflections along the layer lines in the resting and contracting patterns. These two layer lines became slightly sharper in the axial direction but did not shift their peak positions in the radial and axial directions. Thus, the myosin heads seem to geometrically mark the actin filaments during contraction; however, we do not yet have any strong evidence for the labeling of myosin heads to actin following the actin symmetry, as discussed below.

In a rigor muscle, the actin layer-line intensities seemed, in general, to be greater than in the contracting muscle and most of the peaks shifted towards the meridian. The whole pattern had a ladder-like appearance with a strong first layer line at ~1/37 nm^{-1}. This pattern has been shown to arise from a periodic attachment of myosin heads to actin with the symmetry of the actin filament (*7, 23–25*). Thus, the time-averaged structure of the actin filament during steady isometric tension was distinctly different from that of the actin filament in rigor.

The intensification of the actin layer lines remained for the stretched muscle with a small overlap of the thin and thick filaments. This intensity change seemed to be larger than expected, given that the change occurs proportionally to the number of myosin heads that were present in the overlap zone. We also observed that the actin layer lines continued to become more intense further up to the reflection at ~1/1.8 nm^{-1}. Theoretical models have suggested that the intensities of the outer layer lines that appear centered at n/5.4 nm^{-1} (where n = 1, 2, or 3) depend on the shape and orientation of the actin subunits (*22, 26–28*). Recent time-resolved studies have shown that the intensity changes of the 5.9-nm and second layer-line reflections preceded those of the myosin and equatorial reflections on activation (*3, 5, 6*). Taken together, there could also be a change in the structure of the actin monomer itself that takes place in the

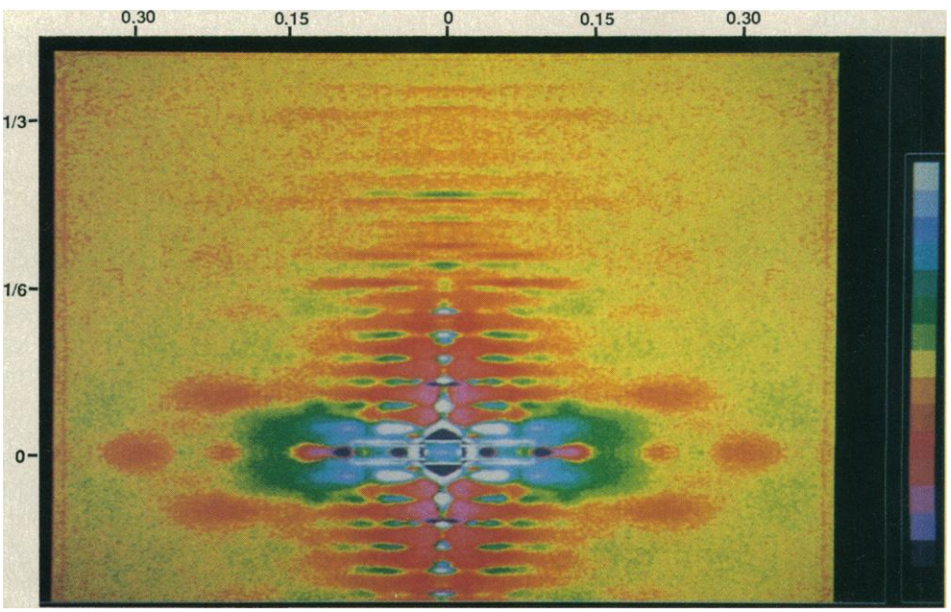

Fig. 3. A difference pattern obtained by subtracting the digital data of the resting pattern (Fig. 2A) from those of the contracting pattern (Fig. 2B). Numbers on the top and left-hand side are reciprocal radial and axial coordinates (in nm^{-1}), respectively. The yellow (0 level) through red to dark violet colors indicate increasing intensities of layer-line reflections and the light green to white colors indicate the decreasing reflection intensities during contraction. Almost all actin-based layer lines increased in intensity. Intensified broad reflections on the row lines at reciprocal radial spacings around 0.15 to 0.3 nm^{-1} between the first and the 2.7-nm layer lines were 11-, 8.6-, and 7.1-nm layer lines, the reflection on the 5.1-nm layer line, 3.9- and 3.0-nm layer-line reflections. The dark violet reflections on the equator and the meridian are the (1,1) and about (4,0) equatorial Bragg reflections and the 14.5-nm myosin meridional reflection, respectively. At radial positions of 0.22 nm^{-1} and 0.32 nm^{-1} on the equator, broad (unsampled) reflections were intensified. The cause of intensification of these equatorial reflections is unknown, but the time course of the intensity change of the reflection at 0.22 nm^{-1} was close to those of the (1,1) equatorial and the 42.9-nm myosin reflections (*5, 6*). Digital recordings of the x-ray patterns stored on magnetic tape were processed by a computer (FACOM, M360) at the Photon Factory and treated with an NEC ACOS 850 computer at the Protein Research Institute of Osaka University. The difference pattern made with an NEC PC-98XA personal computer was transformed into separate red-green-blue data with a contrast ratio of 256 to 1. The gray image for each color was reproduced on the plane cathode-ray tube and the final color photograph was made by exposing each image through RGB filters.

process of activation by an interaction with the myosin heads, as well as by the structural changes of regulatory proteins. This might contribute to the intensity enhancement of the actin layer lines during contraction (*28*).

Changes of the myosin layer lines during contraction. Off-meridional parts of the myosin layer lines and many so-called forbidden meridional reflections decreased greatly in intensity or disappeared. However, the 42.9-nm first off-meridional reflection seemed to remain with about 20 percent of the resting intensity (*2*). The meridional reflections indexed to $3n$ orders of the 42.9-nm repeat were strong up to the 24th one, with a 1 to 3 percent increase in the axial spacing, although the 18th and 21st reflections disappeared. The widths of these reflections perpendicular to the meridian approximately doubled. If the widths were taken into account (*2*), the intensities of most of these reflections even increased, indicating a strengthening of the threefold screw symmetry of the myosin filament (*29*) and a better ordering of myosin projections in planes with an axial spacing of 14.5 nm. In a rigor muscle, these meridional reflections could still be observed, but were weakened; the 42.9-nm layer line completely disappeared. Another feature was that the diffuse small-angle scattering in the central region in the difference pattern of Fig. 3 seemed to be intensified in an approximately elliptic shape that was longer in the axial direction. In agreement with observations from electron microscopic studies of rapid-frozen sample (*30*), our results suggest that, during contraction, the myosin heads retain the axial periodicity of the myosin filament and align more perpendicularly along the actin filaments.

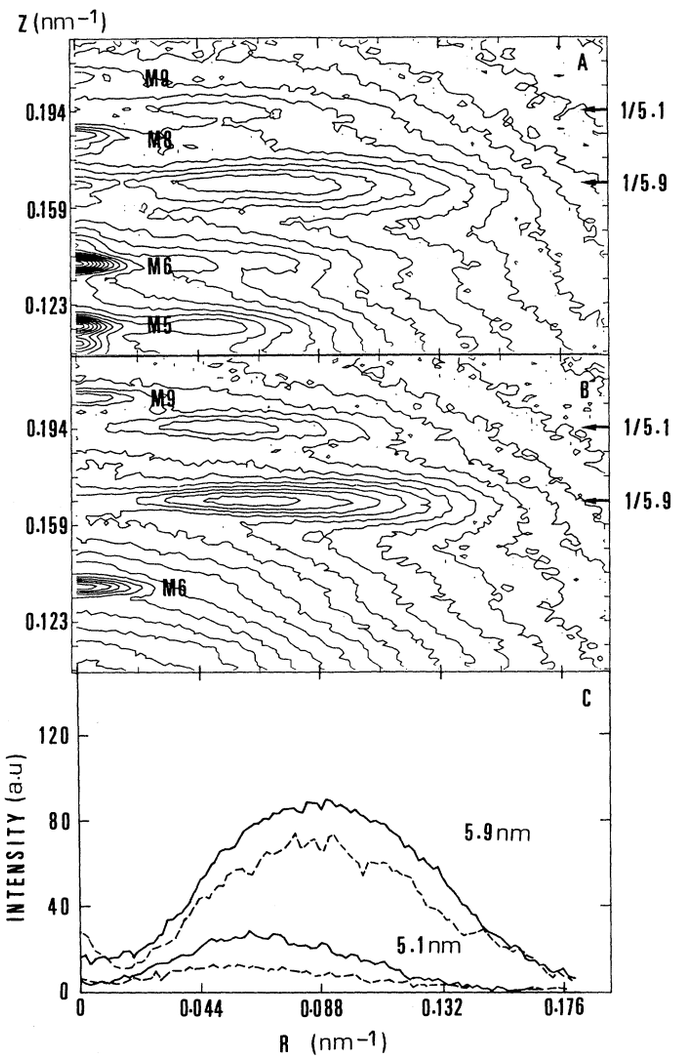

Fig. 4. Intensity contour maps around the 5.9-nm and 5.1-nm actin layer lines (indicated by arrows). (**A**) Resting state; (**B**) contracting state. The contour is drawn at intervals of 0.2 times the square root of the intensity. The intensities (I) were derived from the digital data (D) of the IP with the relation, $I \propto 10^{3.6D/256}$ (*15*). Z is the reciprocal-space axial coordinate from the equator. M5 to M9 are myosin meridional reflections indexed to the fifth to ninth orders of a 42.9-nm repeat. (**C**) Intensity profiles (in arbitrary units) of the 5.9- and 5.1-nm actin reflections. Dashed curves, resting state; solid curves, contracting state. Intensity distributions were measured by scanning the intensity data perpendicular to the layer lines at intervals of 0.4 mm. The area of the peak above the background was adopted as an integrated intensity and plotted as a function of the reciprocal-space radial coordinate (R) from the meridian.

Prospects. The exposure time needed for the recording of the diffraction patterns from muscles when imaging plates are used can be reduced to several milliseconds as more intense x-rays become available from the insertion devices that are expected to be installed in a planned 6- to 8-GeV storage ring. The imaging plate has no counting-rate limitation; thus, it can fully utilize intense x-rays without any counting loss. Time-resolved studies of two-dimensional diffraction patterns should also become possible with a time resolution of less than 1 second by making a device that can rapidly move the imaging plates. Such a technique should provide further insights into the molecular mechanism of muscle contraction as well as insights applicable to kinetic studies in structural biology and high polymer science.

REFERENCES AND NOTES

1. H. E. Huxley, A. R. Faruqi, J. Bordas, M. H. J. Koch, A. R. Milch, *Nature (London)* **284**, 140 (1980); H. E. Huxley, A. R. Faruqi, M. Kress, J. Bordas, M. H. J. Koch, *J. Mol. Biol.* **158**, 637 (1982).
2. H. E. Huxley *et al.*, *Proc. Natl. Acad. Sci. U.S.A.* **78**, 2297 (1981); H. E. Huxley *et al.*, *J. Mol. Biol.* **169**, 469 (1983).
3. K. Wakabayashi *et al.*, *Biophys. J.* **47**, 847 (1985).
4. K. Wakabayashi *et al.*, *ibid.* **49**, 581 (1986); H. Tanaka, T. Kobayashi, Y. Amemiya, K. Wakabayashi, *Biophys. Chem.* **25**, 161 (1986).
5. M. Kress, H. E. Huxley, A. R. Faruqi, J. J. Hendrix, *J. Mol. Biol.* **188**, 325 (1986).
6. K. Wakabayashi, Y. Amemiya, H. Tanaka, in *Actin: Structure and Functions, Proceedings of the 11th Taniguchi International Symposium on Biophysics*, 11 to 16 November 1985, T. Yanagida, Ed. (Taniguchi Foundation, Osaka, 1986), pp. 56–62.
7. H. E. Huxley and W. Brown, *J. Mol. Biol.* **30**, 383 (1967).
8. G. F. Elliott, J. Lowy, B. M. Millman, *ibid.* **25**, 31 (1967).
9. J. C. Haselgrove, *ibid.* **92**, 113 (1975).
10. R. T. Tregear, J. R. Milch, R. S. Goody, K. C. Holmes, C. D. Rodger, in *Cross-Bridge Mechanism in Muscle Contraction*, H. Sugi and G. H. Pollack, Eds. (Univ. of Tokyo Press, Tokyo, 1979), pp. 407–423.
11. I. Matsubara, N. Yagi, H. Miura, M. Ozeki, T. Izumi, *Nature (London)* **312**, 471 (1984).
12. H. E. Huxley *et al.*, in Y. Maeda, in *Structural Biological Applications of X-Ray Absorption, Scattering, and Diffraction*, H. D. Bartunik and B. Chance, Eds. (Academic Press, New York, 1986), pp. 219–234; A. R. Faruqi, H. E. Huxley, M. Kress, *Nucl. Instrum. Methods* **A252**, 234 (1986).
13. M. Sonoda, M. Takano, J. Miyahara, H. Kato, *Radiology* **148**, 833 (1983); H. Kato, J. Miyahara, M. Takano, *Neurosurg. Rev.* **8**, 53 (1985).
14. K. Takahashi, K. Kohda, J. Miyahara, *J. Lumn.* **31, 32**, 266 (1984); K. Takahashi, J. Miyahara, Y. Shibahara, *J. Electrochem. Soc.* **132**, 1492 (1985).
15. J. Miyahara, K. Takahashi, Y. Amemiya, N. Kamiya, Y. Katow, *Nucl. Instrum. Methods* **A246**, 572 (1986).
16. The spatial resolution of the IP is in the end, limited by the thickness of the phosphor layer. For details, see Y. Amemiya *et al.*, in preparation.
17. J. C. Dainty and R. Shaw, *Image Science* (Academic Press, New York, 1974), pp. 28–31.
18. Y. Amemiya *et al.*, *Photon Factory Activity Report* **3**, 265 (1986); Y. Amemiya *et al.*, *Proceedings of the International Conference on Biophysics and Synchrotron Radiation*, Frascati, 14–16 July 1986, A. C. Castellano and L. Invidia, Eds. (Springer-Verlag, Berlin, in press).
19. Y. Amemiya *et al.*, *Nucl. Instrum. Methods* **208**, 471 (1983); K. Wakabayashi *et al.*, in *X-Ray Instrumentation for the Photon Factory: Dynamic Analyses of Micro Structure in Matter*, S. Hosoya, Y. Iitaka, H. Hashizume, Eds. (KTK Science, Tokyo, 1986), pp. 61–74.
20. A freshly dissected sartorius muscle of the bullfrog (*Rana catesbeiana*) was held vertically in a specimen chamber by clamping the pelvic bone at the bottom end and connecting the tibial end to a force transducer (Shinkoh, model UT). Oxygenated Ringer solution (115 m*M* NaCl, 2.5 m*M* KCl, 1.8 m*M* $CaCl_2$, *p*H adjusted to 7.2 with $NaHCO_3$) was continuously perfused through the specimen chamber. The temperature was kept at 6°C. The muscle was isometrically stimulated at a sarcomere length of 2.4 μm for 1.3 seconds through a multi-electrode assembly in the chamber with trains of supramaximal rectangular pulses (3-msec duration at 25 Hz). To record a contracting pattern, this was repeated 10 times at intervals of 15 seconds. A mechanical shutter placed in front of the specimen was synchronously

opened for 1.0 second when a steady tetanic tension had developed to let the x-rays pass through only during the plateau phase of isometric tension. The plateau tension of the 10th contraction was 83 percent of the initial tension. To record the resting pattern before contraction, a 1.0-second exposure was repeated 10 times every 2 seconds by opening the shutter without stimuli to the muscle.
21. H. E. Huxley, *Cold Spring Harbor Symp. Quant. Biol.* **37**, 361 (1972); J. C. Haselgrove, *ibid.* **37**, 341 (1972); D. A. D. Parry and J. M. Squire, *J. Mol. Biol.* **75**, 33 (1973).
22. P. J. Vibert, J. C. Haselgrove, J. Lowy, F. R. Poulsen, *J. Mol. Biol.* **71**, 757 (1972).
23. J. Wray, P. J. Vibert, C. Cohen, *ibid.* **124**, 501 (1978).
24. K. Namba, K. Wakabayashi, T. Mitsui, *ibid.* **138**, 1 (1980).
25. K. C. Holmes, R. T. Tregear, J. Barrington Leigh, *Proc. Roy. Soc.* **B207**, 13 (1980).
26. Y. Tajima, K. Kamiya, T. Seto, *Biophys. J.* **43**, 335 (1983).
27. E. H. Egelman and D. J. DeRosier, *J. Mol. Biol.* **166**, 623 (1983); E. H. Egelman, *J. Muscle Res. Cell Motility* **6**, 129 (1985).
28. The difference cylindrically symmetrical Patterson function (*23*) was calculated from the observed actin layer-line intensity data during contraction. The overall appearance in the map was different from that in the rigor map and similar to that in the map of the smooth muscle thin filament derived by Tajima *et al.* (*25*). We could not detect a distinct contribution from myosin heads. Our calculations revealed that the intensity change of most of the actin layer lines during contraction could be interpreted as a change in the structure of actin monomers as well as the position of tropomyosin molecules in the thin filament. See K. Wakabayashi *et al.*, Proceedings of the Symposium on the Molecular Mechanism of Muscle Contraction, Hakone, 27 to 31 October 1986, H. Sugi and G. H. Pollack, Eds. (Plenum, New York, in press).
29. N. Yagi, E. J. O'Brien, I. Matsubara, *Biophys. J.* **33**, 121 (1981).
30. S. Tsukita and M. Yano, *Nature (London)* **317**, 182 (1985).
31. H. E. Huxley and A. R. Faruqi, *Annu. Rev. Biophys. Bioeng.* **12**, 381 (1983).
32. We thank T. Kobayashi, H. Iwamoto, T. Hamanaka, A. Fujishima, and J. Kurihara for assistance with the experiments; K. Takahashi, N. Mori, and H. Ayato for discussions and kind help about the use of the SLSL system; J. Chikawa, T. Matsushita, T. Mitsui, and H. Sugi for their encouragement; N. Tanaka for his advice on data treatment; T. Minami for reproduction of the difference image; and T. Yanagida for critical reading of the manuscript. Partially supported by a grant-in-aid for scientific research (No. 60480512) and a grant-in-aid for special project research (No. 61230015) (K. Wakabayashi) and a grant-in-aid for developmental scientific research (No. 60850013) (J. Chikawa) from the Ministry of Education, Science and Culture, Japan.

19 December 1986; accepted 18 May 1987